Seabed erosion on the Lomonosov Ridge, central Arctic Ocean: A tale of deep draft icebergs in the Eurasia Basin and the influence of Atlantic water inflow on iceberg motion?

Y. Kristoffersen,[1] B. Coakley,[2] W. Jokat,[3] M. Edwards,[4] H. Brekke,[5] and J. Gjengedal[1]

Received 14 November 2003; revised 19 April 2004; accepted 6 May 2004; published 6 August 2004.

[1] The submarine Lomonosov Ridge, which bisects the Arctic Ocean, is covered by ~450 m of hemipelagic sediments. High-resolution chirp sonar and side-scan data have documented erosion of a section of the ridge. Here we present multichannel seismic and chirp sonar data which show removal of unconsolidated sediments along the Eurasia Basin side of the Lomonosov Ridge, where the central ridge is shallower than 1000 m. The incomplete erosion of the hemipelagic drape and probable topographic control of ice motion suggest that the deepest draft glacier ice, which reached the central Arctic Ocean from the Eurasia Basin, was in the form of armadas of large icebergs embedded in sea ice rather than a single, continuous floating ice shelf. Massive, rapid discharge of glacier ice was probably required to produce the deepest draft (>800 m) icebergs. Eastward and northward drift trajectories from a likely iceberg source area on the Kara-Barents Sea margin would reflect the relative strength of Atlantic inflow through the Fram Strait. However, only icebergs with drafts exceeding bathymetric thresholds on the Lomonosov Ridge would leave an erosive imprint on the seabed. Advection of Atlantic water may have been relatively strong at times of discharge from the Saalian ice sheet. Icebergs exiting the Arctic Ocean caused massive erosion and redeposition of the hemipelagic sediments on top of Yermak Plateau. *INDEX TERMS:* 3309 Meteorology and Atmospheric Dynamics: Climatology (1620); 4207 Oceanography: General: Arctic and Antarctic oceanography; 4215 Oceanography: General: Climate and interannual variability (3309); *KEYWORDS:* Arctic Ocean, paleoclimate, Atlantic Water inflow, icebergs, ice drift, seabed erosion

Citation: Kristoffersen, Y., B. Coakley, W. Jokat, M. Edwards, H. Brekke, and J. Gjengedal (2004), Seabed erosion on the Lomonosov Ridge, central Arctic Ocean: A tale of deep draft icebergs in the Eurasia Basin and the influence of Atlantic water inflow on iceberg motion?, *Paleoceanography*, *19*, PA3006, doi:10.1029/2003PA000985.

1. Introduction

[2] The question of the thickness and extent of a marine ice cover in the north polar basin during glacial extremes is important for our understanding of the relation between sea level, oxygen isotopes, and global ice volume [*Broecker*, 1975; *Williams et al.*, 1981; *Shackleton*, 1987]. It also relates to the variation in inflow of warm Atlantic water during glacial/interglacial cycles as well as the stability of former ice sheets on the circum-Arctic shelves and continental hinterland.

[3] During glacial maxima, the Arctic Ocean was surrounded by large continental ice sheets on North America, Europe, and the Russian arctic margins. Floating ice shelves more than 1 km thick have been postulated in the polar basin [*Mercer*, 1970; *Hughes et al.*, 1977; *Grosswald and Hughes*, 1999], while most workers [*Clark*, 1990; *Ishman et al.*, 1996; *Bischof and Darby*, 1997; *Philips and Grantz*, 2001] believe the sea ice cover was much like the present day, consisting of seasonal sea ice. Thick glacial ice in the Arctic Ocean would have shaped the seafloor down to its maximum draft. Evidence of seabed forms sculpted by glacier ice have been observed in water depths down to 500 m on the Chuckchi borderland, to 950 m on the Lomonosov Ridge [*Polyak et al.*, 2001], and to 850 m on the Yermak Plateau [*Vogt et al.*, 1994]. *Vogt et al.* [1994, p. 406] suggested that "calving marine ice shelves up to 500–700 m thick were present in the Arctic Ocean upstream from the Yermak area, with an ice rise 400–600 m thick grounded on the plateau crest," while *Polyak et al.* [2001] consider a fluted and eroded seabed across the Lomonosov Ridge crest as an indicator of active grounded ice flow in the direction toward Alaska rather than footprints of single large icebergs.

[4] The seismic reflection data presented here demonstrate that deep draft ice partly removed sediments on the Eurasia Basin flank of Lomonosov Ridge. The most likely cause of the erosion was large single icebergs. Northward drift trajectories from a probable source area at the Kara-Barents Sea margin require forcing from subsurface inflow of Atlantic water to be larger than the combined influence of the flow of surface water and the Transpolar Drift of sea ice. This suggestion is

[1]Department of Earth Science, University of Bergen, Bergen, Norway.
[2]Department of Geology and Geophysics, University of Alaska Fairbanks, Fairbanks, Alaska, USA.
[3]Alfred-Wegener Institute for Marine and Polar Research, Bremerhaven, Germany.
[4]Hawaii Mapping Research Group, Hawaii Institute of Geophysics and Planetology, University of Hawaii, Honolulu, Hawaii, USA.
[5]Norwegian Petroleum Directorate, Stavanger, Norway.

0883-8305/04/2003PA000985$12.00

compatible with a growing body of evidence for advection of Atlantic water along the northern Kara-Barents Sea margin of the Arctic Ocean at least throughout the middle to late Pleistocene [*Hevrøy et al.*, 1996; *Knies et al.*, 2000; *Spielhagen et al.*, 2004].

2. Materials and Methods

[5] Multichannel seismic reflection profiles across Lomonosov Ridge and Yermak Plateau acquired by icebreakers *Polarstern* in 1991 and *Oden* in 1996 and 2001 are the primary data sets for studies of the upper 1 km of the acoustic stratigraphy. During SCICEX 1998 and 1999, the shallow strata (upper +50 m) were imaged by chirp subbottom profiler and the seafloor surface was imaged with a side-scan sonar system. These data were acquired by U.S. Navy nuclear submarine *Hawkbill* [*Polyak et al.*, 2001]. The experimental setup in practical multichannel seismic data acquisition by a single icebreaker in heavy ice limits the receiver to a short hydrophone cable (2–300 m, 8–12 channels) towed 100–150 m behind the vessel. The seismic source used on Lomonosov Ridge consisted of two 1.3 L air guns, while lighter ice conditions on Yermak Plateau permitted use of a cluster of eight 1.3 L guns in 1991 and two 3 L GI guns in 2001. Seismic data south of 81° N were obtained under regular open water conditions [*Sundvor et al.*, 1982]. The seismic data acquired by icebreakers in a crooked line geometry were edited, bandpass filtered, and sorted in to common midpoint bins at 25 m intervals. Stacking velocities were adapted from sonobuoy measurements. The quality of the final processed seismic sections is surprisingly good, although the frequency content and signal to noise ratios vary considerably due to variations in source and receiver depths forced by changes in the speed of advance through the ice.

[6] The reflection hyperbolas recorded from sonobouy measurements corrected for nonlinear increase in offset were used to calculate seismic velocities within the upper kilometer of the subbottom sediments. Three sonobuoys were deployed on Lomonosov Ridge (line AWI 91090) and four on northern Yermak Plateau (line NPD 0101), respectively.

[7] The high-resolution chirp subbottom profiler use a 50 ms long sweep (2.7–6.7 kHz), which yields a vertical resolution of 0.3 m and more than 50 m of penetration in soft hemipelagic sediments. The side-looking sonar was a SeaMARC™ type. The swath data were processed at the Hawaii Mapping Research Group.

3. Results

3.1. Evidence of Depth-Dependent Erosion on Lomonosov Ridge

[8] The Lomonosov Ridge has the dimensions of a submarine alpine mountain chain rising more than 3 km above the abyssal plain. Only isolated areas are shallower than 1 km (Figures 1 and 2). In most places the ridge is capped by a ~450 m hemipelagic sediment drape above an erosional unconformity [*Jokat et al.*, 1992]. However, along the shallowest part of the crest (84°30′–87°30′N) facing the Eurasia Basin, the upper part of the sediment drape is partly removed (Figures 1–3c). In Figures 3a and 3b we illustrate the contrast between:

[9] 1. The uniform character of the undisturbed hemipelagic drape across Lomonosov Ridge below 1000 m water depth (line AWI91090).

[10] 2. A case where the ridge crest is bevelled to a maximum depth of ~980 m (*Hawkbill* line 99-I). We assume an average sound velocity in water of 1450 m/s [*Jakobsson*, 1999].

[11] 3. A shallower area where the sediment drape along the Eurasia Basin side is partly disturbed (line UB96012).

[12] 4. The shallowest part of the ridge where the acoustic layering appears truncated at the seabed on the Eurasia Basin side (line UB96015).

[13] The area of truncated acoustic stratification increases in width along the flank of the bathymetric high from about 10 km in the north (Figure 3a, line UB96012) to 15 km farther south (Figure 3a, line UB96015), while the water depth of the cut-out terrace shallows by about 150 m and the ridge crest proper by about 200 m. Seabed within the relatively flat part of the terrace appears smooth with conformable subbottom acoustic interfaces at the resolution of multichannel seismic data. However, the high-resolution chirp data demonstrate fine-scale acoustic stratification truncated at the seabed (Figure 3c; *Hawkbill* 99-D1 and -D2). The seabed on the adjacent higher slope is more hummocky and a SCICEX side-scan image (shown in the work of *Jakobsson* [2000]) reveals abundant subparallel furrows which appear to be aligned with the ridge crest topography rather than crossing it (Figure 2).

3.2. Evidence of Depth-Dependent Erosion on Yermak Plateau

[14] Yermak Plateau partly occludes the exit for deep draft ice export from the Arctic Ocean (Figure 1). The present plateau morphology is characterized by a bevelled crest with slightly steeper slope along the western side of the N-S trending part of the plateau (Figures 4 and 5). At ~820 m present water depth we observe a transition from a relatively smooth seabed on the middle continental slope to a more undulating bottom at shallower depths on the western side (Figure 5, line AWI91128-31). Plowmarks are present along the crest and eastern slope of southern Yermak Plateau down to over 850 m water depth [*Vogt et al.*, 1994]. New SCICEX side-scan sonar images from water depths greater than 850 m on the northern part of the plateau image abundant plowmarks in the seabed (Figure 6). A depth consistent transition in seabed morphology can be followed along the slope west of Svalbard at least down to 78° N (Figure 4), but is not apparent on the slope north of Svalbard east of about 15°E.

[15] Massive erosion of the crestal region (shallower than 850 m) of Yermak Plateau is documented in the seismic reflection data (Figure 5). On the northern part of the plateau, acoustically well-stratified, low-velocity (1.7 km/s) strata are cut by a seabed-parallel unconformity at ~830 m below present sea level (Figure 5, line NPD0101). The overlying 40–80 m thick sediments are acoustically incoherent, suggesting disturbed stratification. The unconformity surface varies with local depressions of

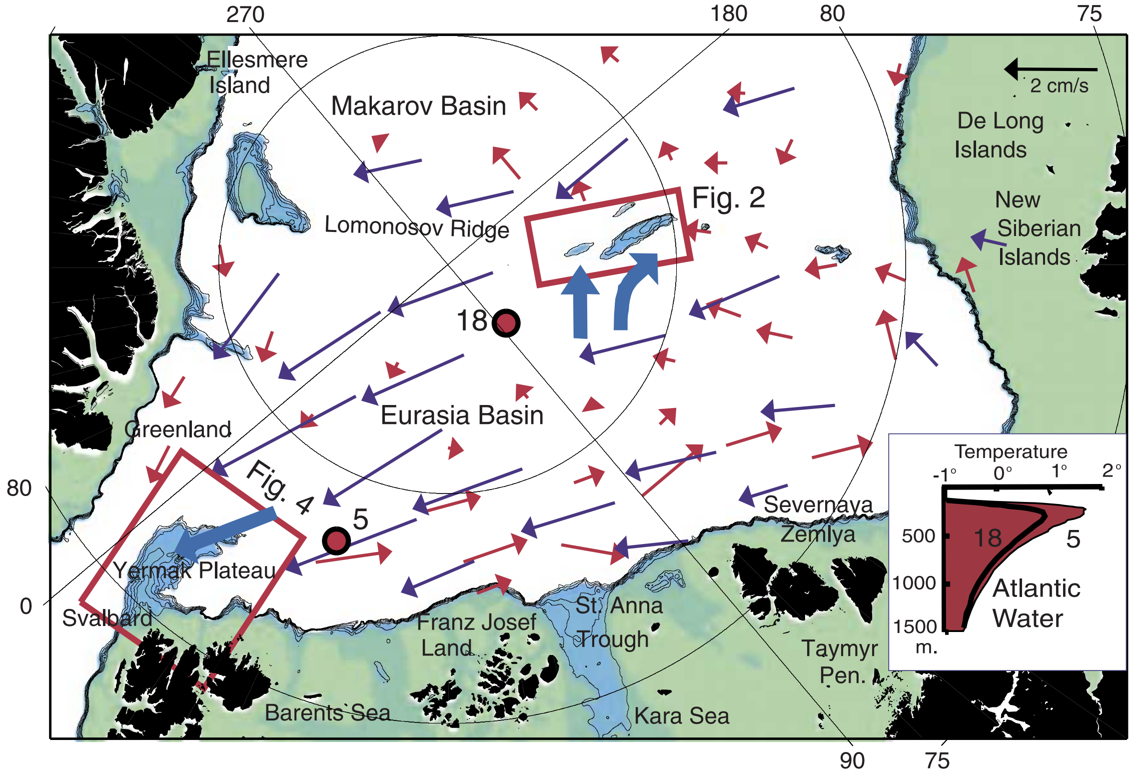

Figure 1. Map of Eurasia Basin, Arctic Ocean [*Jakobsson et al.*, 2000] with water depths shallower than 1000 m color-coded, representing areas potentially affected by the deepest draft icebergs. Present pattern of sea ice drift (thin blue arrows) from the International Arctic Buoy Program [*Rigor et al.*, 2002]. Computed current velocities in the Atlantic layer at 500 m depth (red arrows) are from *Zhang et al.* [1998], who used a coupled ice-ocean model forced by observed sea level pressures and surface air temperatures. Right insert shows temperature profiles from *Rudels et al.* [1994] at stations 5 and 18 which, indicate the depth range of Atlantic Water in the Eurasia Basin. The drift directions of the deepest draft icebergs as derived from seabed erosion are shown by thick blue arrows.

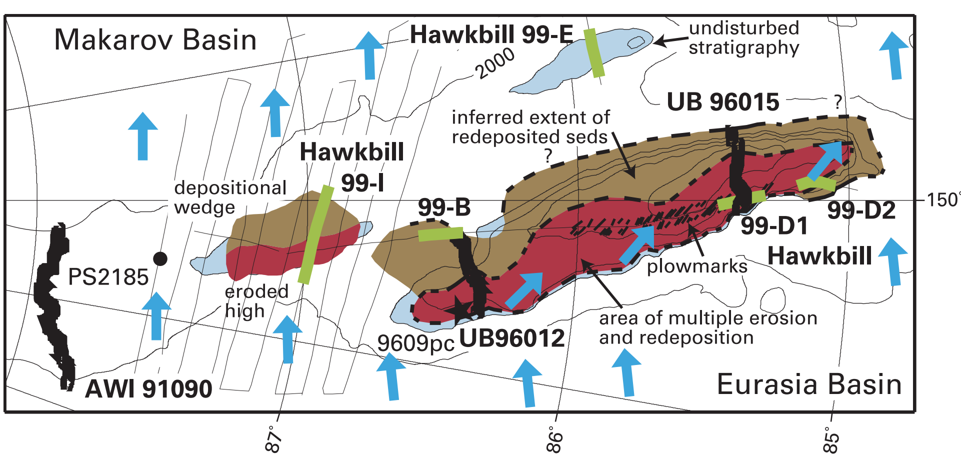

Figure 2. Bathymetry of the central part of Lomonosov Ridge (water depths shallower than 1000 m; blue color with 50 m contour interval) with inferred drift pattern of deep draft ice (thick blue arrows). High-resolution seismic chirp sonar (thin black lines) and multichannel seismic data (heavy black lines) have been used to map out areas of erosion (red) and deposition (brown). Sections of multichannel seismic (heavy black lines) and chirp sonar profiles (heavy green lines) are shown in Figures 3a–3c). Location of a sediment core with report of overconsolidated sediments by *Jakobsson et al.* [2001] is indicated by star. The location of core PS2185 deeper than the maximum erosion level [*Evans and Kaminski*, 1998; *Spielhagen et al.*, 2004] is shown by a filled circle.

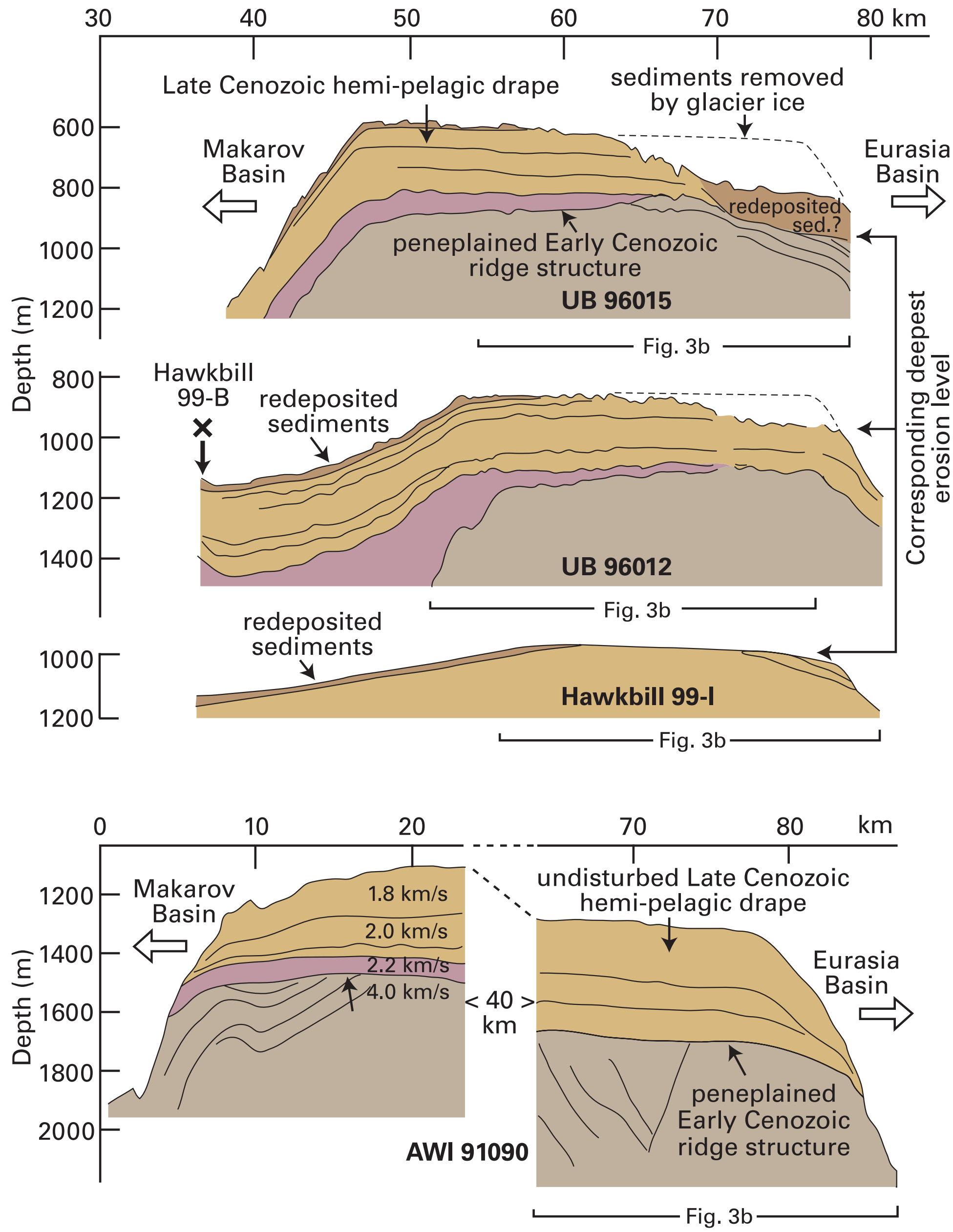

Figure 3a. Line drawing of seismic lines across Lomonosov Ridge. Location of profiles in Figure 2.

similar character as the present seabed. If we assume stratal continuity above the unconformity across the anticline in line NPD0101 (Figure 5), more than 240 m of sediments have been removed. A topographic high at ~81°25′N, 7°E has no sediments on top, but a prograding accumulation along its southwestern side down-lapping on the sediments along the foot of the high (Figures 4 and 5, line UB7908).

[16] Similarly on the southern part of the plateau, up to ~80°30′N, where conventional seismic data acquisition has been possible, we observe an unconformity parallel to the bevelled seabed overlain by a 0–50 m thick acoustically incoherent unit (Figures 4 and 5). The unconformity is documented by the drilling results from Site 910 [*Hull et al.*, 1996] but is less well resolved in the seismic data (Figure 5, line AWI91128-31). Below the unconformity is a westward propagating sediment wedge, which underlies most of the present plateau crest. Strata on the eastern flank in this area become progressively truncated/attenuated upslope. Up to 100 m of section has been eroded off the crest if we assume a straight linear change in sediment thickness between the eastern and western ridge flanks. Drilling into the sediments above the unconformity at the ridge crest (Figure 5, Ocean Drilling Program (ODP) Site 910) suggests continuous sediment deposition of the upper 24 m below the seafloor since marine isotope stage (MIS) 16 [*Hull et al.*, 1996; *Flower*, 1997]. Sediment shear strength increased rapidly

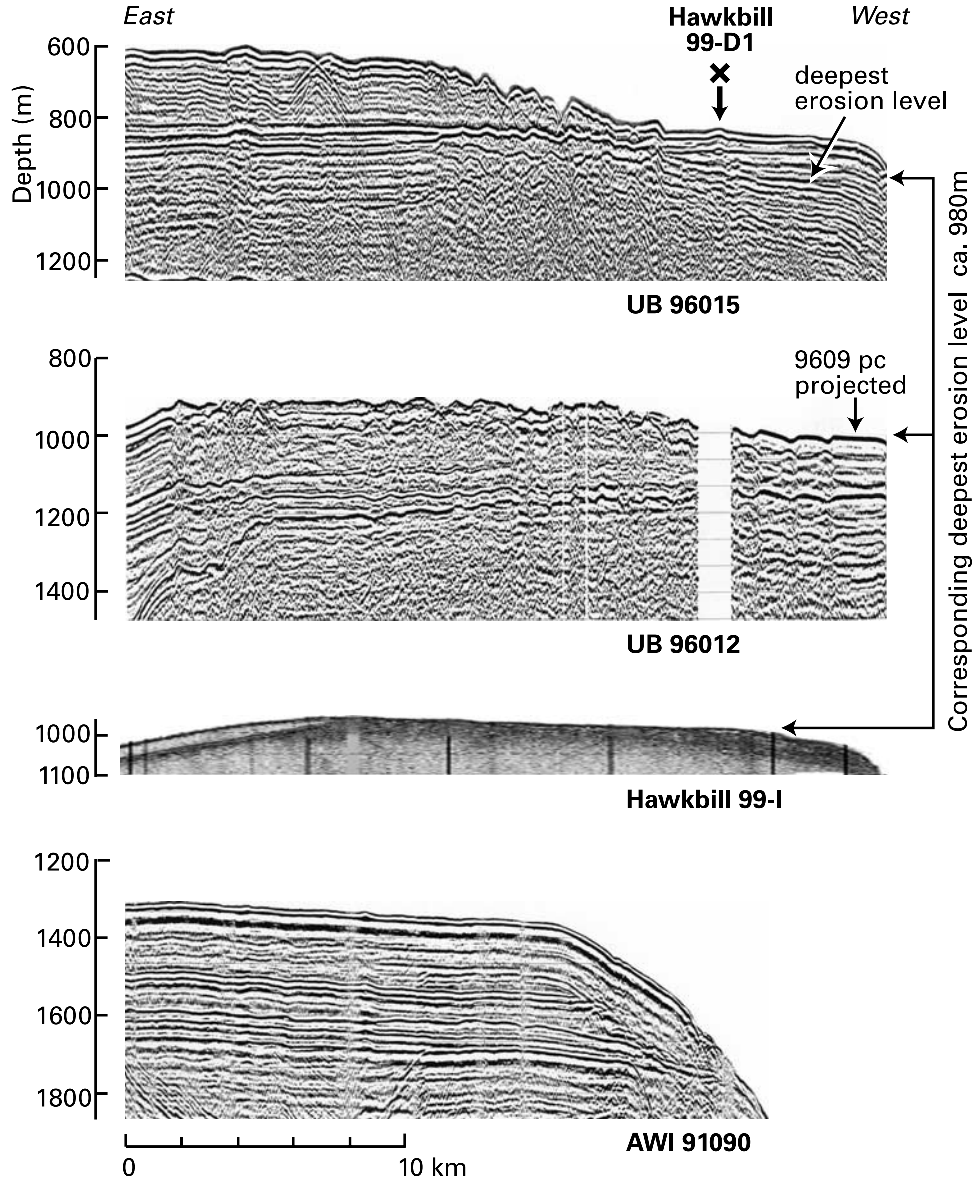

Figure 3b. Sections of multichannel seismic and chirp sonar data across the Eurasia Basin flank of Lomonosov Ridge. Profile locations shown in Figures 2 and 3a.

at 19.5 m subbottom, and the base of the unconsolidated section can only be assumed to be between 70 and 95 m below the seafloor because of recovery problems [*Thiede and Myhre*, 1996]. The sediments are silty clays and clayey silts with >20% siliclastic components and high abundance of dropstones. The Quaternary/Pliocene transition is placed at 67 m subbottom, and the lower part of the Quaternary section appears to be missing [*Hull et al.*, 1996].

[17] The seismic evidence of erosion on Yermak Plateau is supported by drilling results. The apparent transport direction of eroded sediments is from northeast to southwest and similar to the direction of plowmarks found on the present seabed (Figures 4 and 6). Subsequent sediment deposition above the unconformity have been disturbed to create an upper acoustically incoherent unit. We note, however, that studies of the relatively few, short (≤13 m) sediment cores recovered from Yermak Plateau, so far, have not reported on disturbed stratigraphy [e.g., *Bostrøm and Thiede*, 1984; *Aldahan et al.*, 1997].

4. Discussion

4.1. Erosion by Bottom Currents: A Floating Ice Shelf or Deep Draft Icebergs?

[18] The crestal region (<1500 m water depth) of Lomonosov Ridge is within the flow regime of intermediate water mainly derived from inflow of Atlantic water. Contour currents flow toward Greenland on the Eurasia Basin side and toward Siberia on the Makarov Basin side

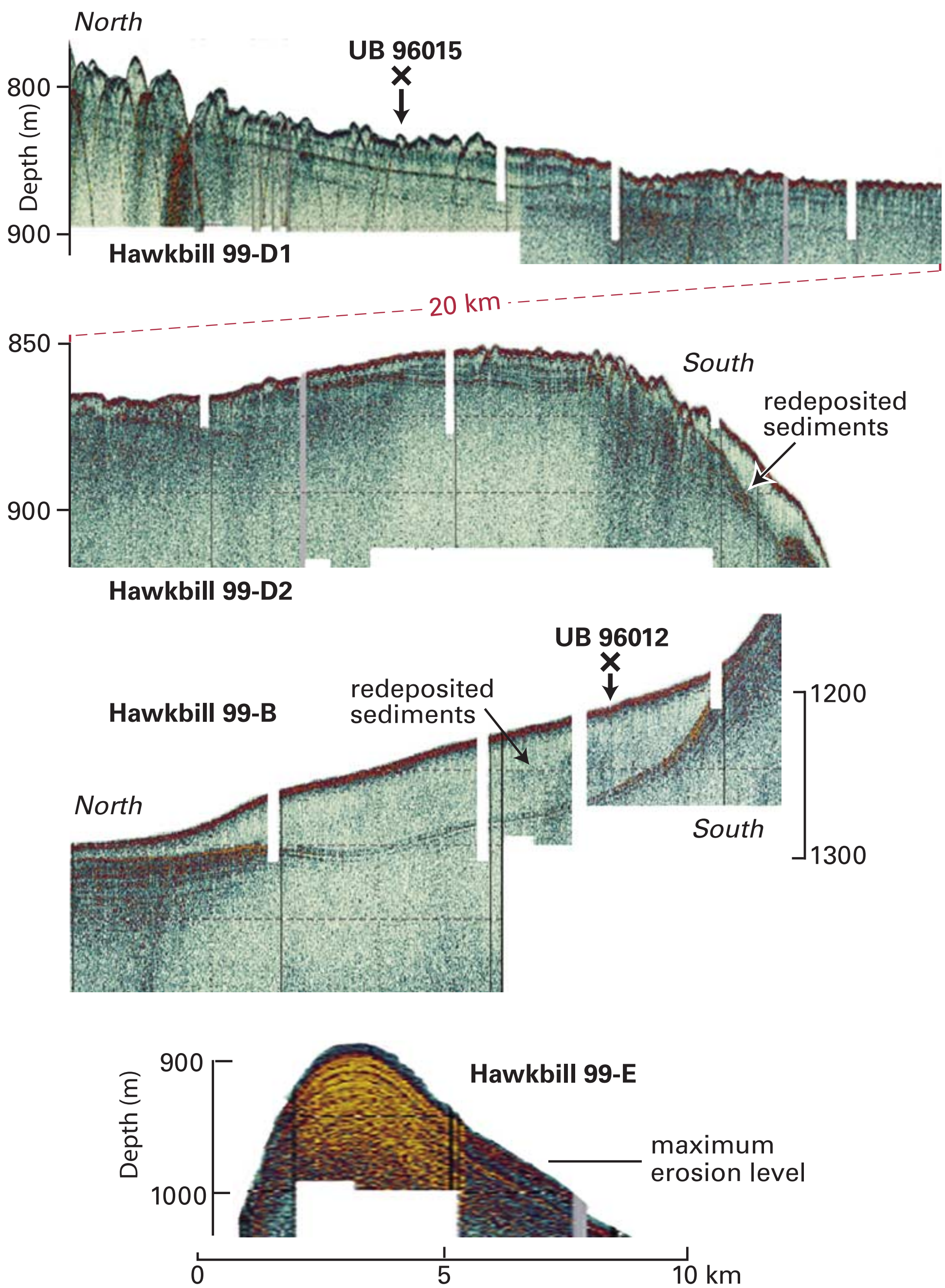

Figure 3c. Sections of chirp sonar data which resolve erosional and depositional features not apparent in the multichannel seismic data. Locations of profiles shown in Figures 2, 3a, and 3b.

[*Rudels et al.*, 1994]. The acoustic stratification displayed in line AWI 91090 shows no evidence of significant current controlled sediment deposition (contourites) in the crestal area of Lomonosov Ridge at ~88°N (Figures 2 and 3a–3b). Measured average current velocities are low (<4 c/m/s with peak values <12 cm/s) along the ridge flank about 300 km farther toward Greenland from our survey area [*Aagard*, 1981]. The observed currents are insufficient to erode cohesive bottom sediments. On the ridge crest 30–40 km from the site of the current measurements, some sediment redistribution is inferred from ripple marks and scouring as well as patches of clean, coarse gravel pavement evident in seabed photographs taken during the drift of ice station LOREX [*Blasco et al.*, 1979]. However, a high-resolution acoustic profile along the LOREX track shows the upper ~75 m of subbottom sediments to be broadly conformable with underlying strata [*Weber*, 1980].

[19] *Polyak et al.* [2001] presented high-resolution (chirp subbottom profiler) seismic data and side-scan seafloor

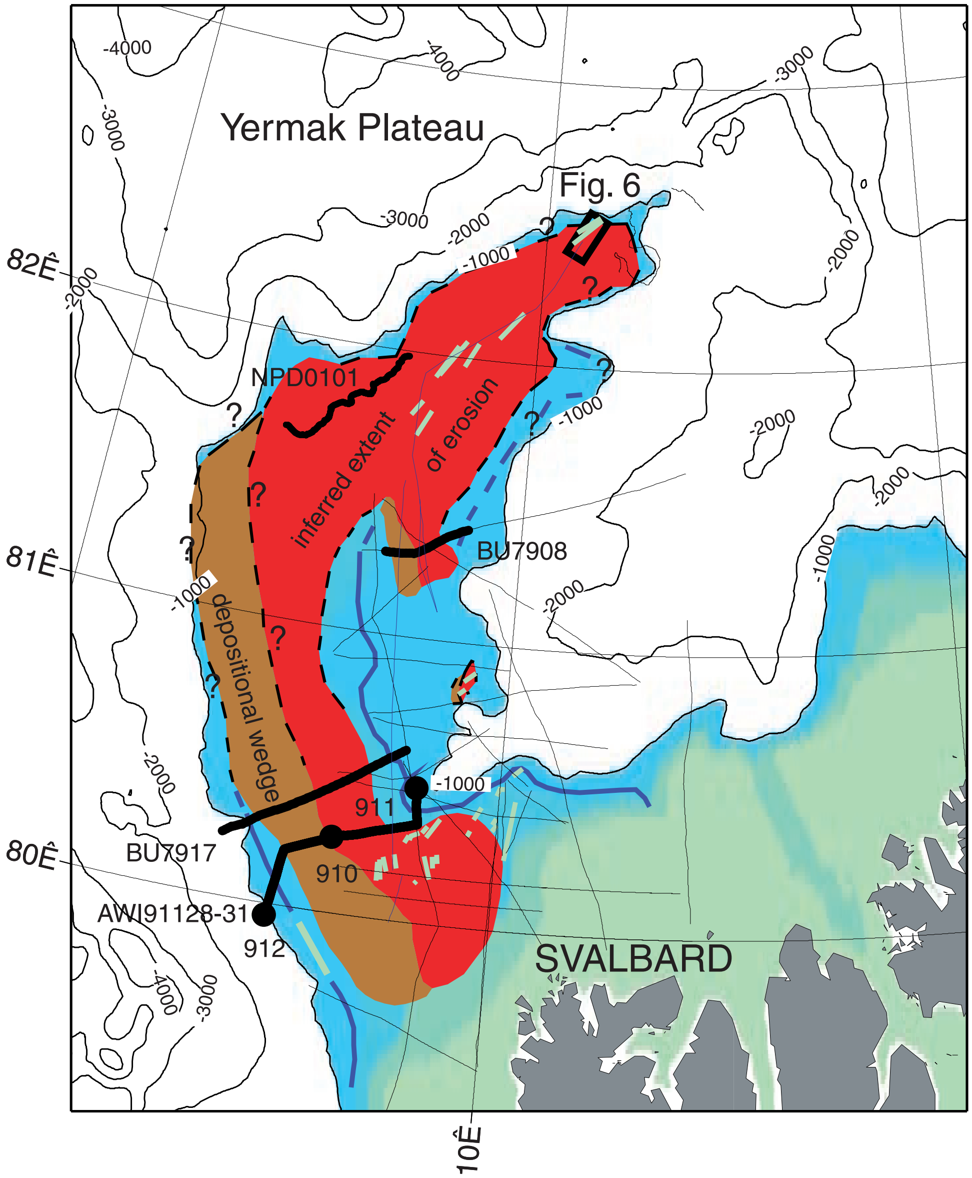

Figure 4. Bathymetry of Yermak Plateau with depths shallower than 1000 m color-coded (light blue less than 1000 m and light green less than 250 m). Areas of iceberg erosion (red) and deposition (brown) are outlined, and the deepest seabed impacts of deep draft ice are indicated by the deep blue line. Short yellow line segments represent iceberg plowmarks in the southern part from *Vogt et al.* [1994] and in the northern part from new SCICEX data (Figure 6). Locations of Ocean Drilling Program Sites 910–912 shown by circles.

images, which display convincing evidence for erosion by deep draft glacier ice across a ~100 km long section (86°45′N–87°25′N) of the ridge crest (Figure 2). This bathymetric high was planed to a maximum erosion level of ~980 m present water depth. An estimated +50 m thick section of hemipelagic sediments was removed. The presence of an adjacent depositional wedge indicates ice motion directly across the ridge crest from the Eurasia Basin toward the Makarov Basin (Figure 2). The authors further interpreted the evenly fluted seabed near the maximum erosion level to reflect the action of a single moving ice massif, while subparallel iceberg scours at shallower water depths (750–950 m) probably indicate flow of megabergs after the major ice shelf disintegration.

[20] The multichannel seismic data across the shallowest part of Lomonosov Ridge (85°–86°30′N) presented here demonstrate depth-dependent erosion limited to the flank facing the Eurasia Basin side (Figures 1–3c). Bedforms within the eroded zone are shown by SCICEX side-scan imagery to comprise subparallel seabed furrows interpreted as iceberg plowmarks [*Jakobsson*, 2000; *Polyak et al.*, 2001]. In addition, overconsolidated (100 kPa) sediments have been recovered within this zone (Figure 2, 9609pc) by piston corer at ~2 m subbottom [*Jakobsson et al.*, 2001].

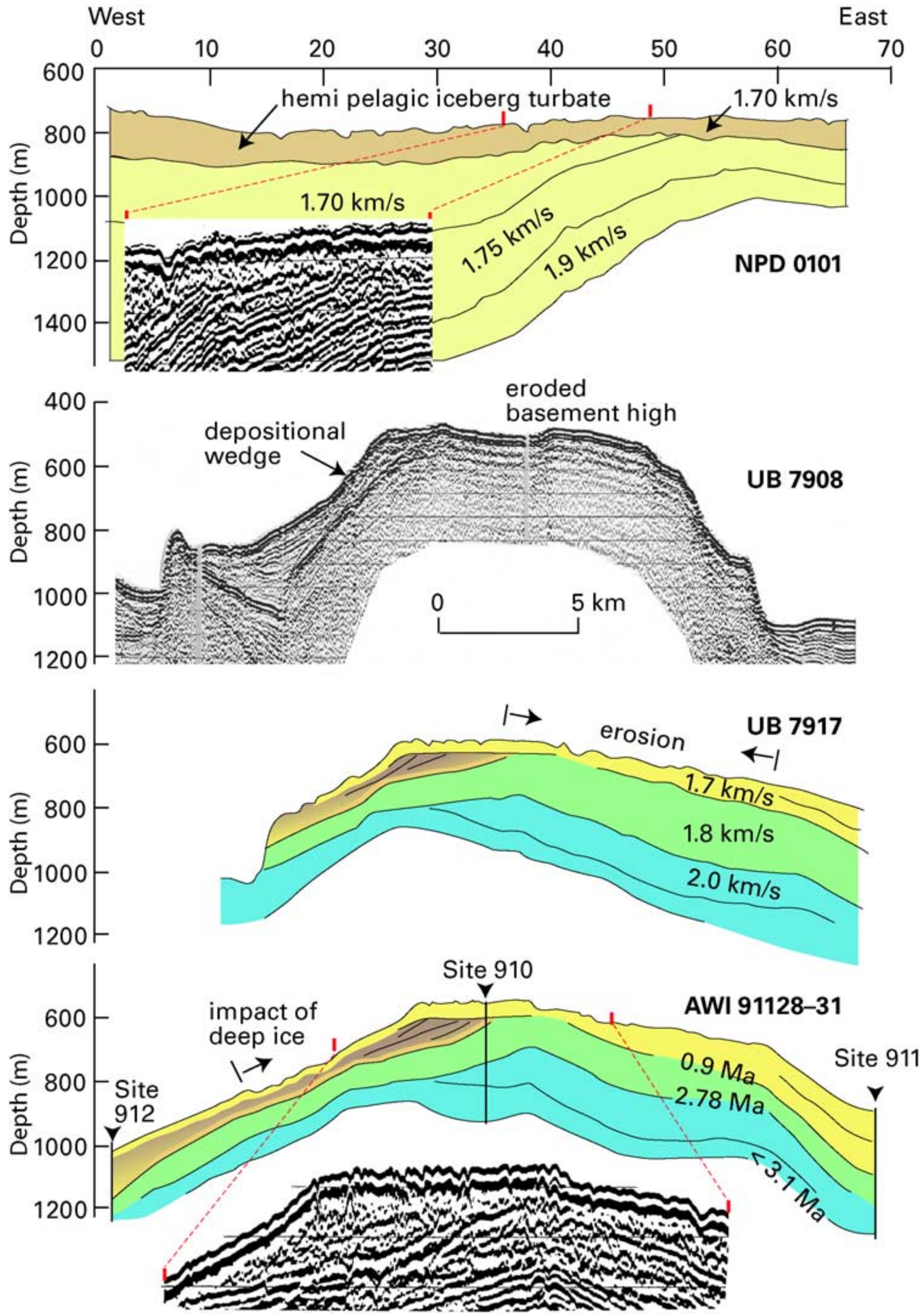

Figure 5. Line drawings and seismic sections across Yermak Plateau. Stratigraphic information on line AWI91128-31 from *Myhre et al.* [1995] and velocity information on line UB7917 from *Austegard* [1982]. Horizontal scale in kilometers on top of figure except for line UB7908. Profile locations are shown in Figure 4.

We suggest that partial erosion of the hemipelagic drape on the shallowest part of Lomonosov Ridge was most likely caused by deep draft ice being diverted by bottom topography. Moving ice bevelled the ridge crest where the original water depth was close to the level of deepest erosion, i.e., at 87°N (Figures 2 and 3a–3c), as pointed out by *Polyak et al.* [2001], but was diverted toward south by the bottom topography where the ridge was shallower (Figure 2). We also note the undisturbed stratigraphy preserved on top of a small bathymetric high at 86°N, 157°E, ~50 km west of the ridge crest proper (Figures 2 and 3c, line *Hawkbill* 99-E) in water depths more than 50 m

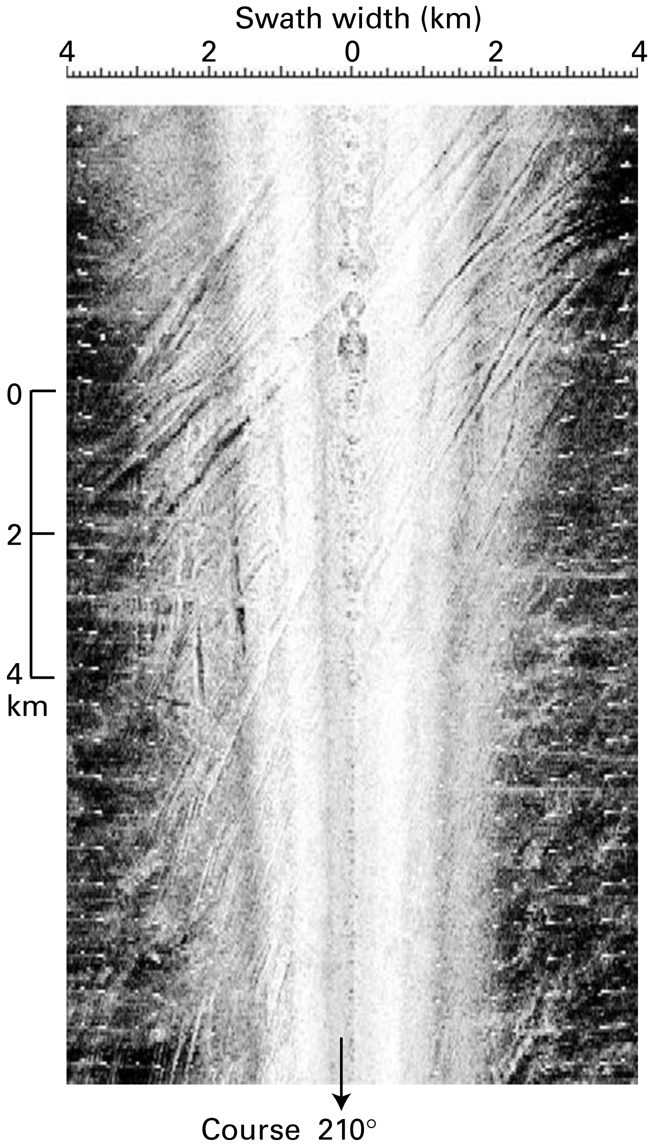

Figure 6. Side-scan sonar image of the seabed on northern Yermak Plateau acquired by U.S. Navy nuclear submarine *Hawkbill*. The water depths vary from 870 m in the top part of the image to 820 m in the lower part.

shallower than the deepest erosion level elsewhere. This observation suggests diversion of the trajectories for the deepest draft ice upstream from this location.

[21] Diverted deep draft ice eroded the Eurasia Basin flank of Lomonosov Ridge and redeposited the sediments downstream along the same flank (Figure 3c, line *Hawkbill* 99-D2). Deep draft ice may initially have cut the Eurasia Basin flank to the same maximum level (Figures 3a and 3b). Later infilling at the southern end of the high was sourced by erosion of shallower topography upstream (Figures 2, 3a, and 3b, line UB96015). Some material was moved across the ridge crest and redeposited along the Makarov Basin flank of the Lomonosov Ridge high. A SCICEX chirp line crossing the eastern end of seismic line UB96012 shows the upper 20–50 m subbottom sediments to be redeposited (Figure 2, line UB96012; Figure 3c, line *Hawkbill* 99-B). A cover of this magnitude is therefore likely to be present on the Makarov Basin flank along the entire length of the high (Figure 2).

[22] The key paleoceanographic question of the glacial Arctic Ocean is the presence and extent of a floating ice shelf. The depth and extent of erosion on the Lomonosov Ridge give evidence of the force applied by the grounded ice. We argue that backstresses in grounded ice on the Eurasia Basin flank of Lomonosov Ridge were relatively small if bottom topography comprising soft hemipelagic drape ($v \leq 2$ km/s) was able to divert motion of more than 800 m thick grounded ice and only suffer partial erosion. Alternatively, the duration of the event(s) were relatively short, but this would seem to be incompatible with an extensive, continuous ice sheet. A numerical modeling experiment also suggests that a floating ice shelf sourced from the Barents and Kara Sea margin will not ground on Lomonosov Ridge even for ultralow basal melt rates unless the strain rate is effectively reduced to zero by a buttress of some sort [*Jakobsson et al.*, 2003]. Sea ice cover may temporarily reduce the tendency for the front of an advancing ice shelf to split up [*Reeh et al.*, 2001], but back pressures generated by sea ice are likely to be insignificant for buttressing an advancing ice shelf which is about two orders of magnitude thicker. If, for some reason, a floating ice shelf thick enough to ground on the central shallowest part of Lomonosov Ridge reached this threshold, we would expect the stream lines to diverge and flow of ice around both sides of the obstacle rather than mainly an apparent southward deflection (Figure 2). Less-obstructed flow of ice immediately to the north of the high was almost due east as seen from the juxtaposition of the eroded area and adjacent depositional wedge at 87°N (Figure 2). Alternatively, the pattern of erosion and redeposition is incompletely mapped. Also, the plowmarks observed on the present seabed could be a late feature as suggested by *Polyak et al.* [2001].

[23] Seabed erosion in the central Arctic Ocean by large icebergs is another possibility. Icebergs with horizontal dimensions of several tens to hundreds kilometers and sufficient draft to ground on Lomonosov Ridge would have an erosive capacity limited by their momentum and the balance of forces acting on their surfaces. Their motion would not be constrained by an adjoining continuum of ice as in the case of a floating ice shelf and thus provide a simpler explanation for the pattern of erosion and the inferred limited backstresses involved. Once topography had been eroded to near the maximum erosion level, the base of a large iceberg and a grounded ice shelf would have the same smoothness to generate a fluted surface as seen by *Polyak et al.* [2001] at 87°N. Smaller icebergs or broken off pieces would have shallower drafts but would be more likely to have protruding keels to generate the furrowed seabed observed at depths shallower than the maximum erosion level [*Polyak et al.*, 2001]. Individual, narrow-keeled icebergs would furrow the seafloor but not create an extensive erosional surface as is observed on the Lomonosov Ridge.

[24] On Yermak Plateau a number of different features reflect iceberg erosion (Figure 4). Iceberg plough marks are

present in the seabed down to 870 m water depth (Figures 4 and 6), and an erosional unconformity has been documented at ODP Site 910 [*Hull et al.*, 1996] as well as overconsolidated sediments in stratigraphically higher positions. The depositional wedges are consistently present along the western slope of bathymetric highs (Figure 4) and suggest erosion by ice exiting the Arctic Ocean.

4.2. Source Area for the Deepest Draft Icebergs in the Polar Basin

[25] The position of the eroded zone and the depth of the unconformity constrain the source and thickness of the ice. In the central Arctic Ocean the deepest draft ice moved across Lomonosov Ridge from the Eurasia Basin to the Makarov Basin (Figure 1). The level of erosion suggests that maximum ice thickness must have been about 900 m, assuming a sea level lowering of ~150 m [*Rohling et al.*, 1998] and a 10% freeboard.

[26] Five glacially eroded troughs are present on the outer Barents Shelf between Svalbard and Severnya Zemlya (Figure 1). Of these, the St. Anna Trough has the largest morphological expression of erosion by glacier ice on the entire circum-Arctic margin [*Cherkis et al.*, 1991; *Jakobsson et al.*, 2000]. It is of similar dimensions as the Bear Island Trough on the western Barents shelf but is more than150 m deeper. The past depth profile of St. Anna Trough may differ from the present, which is partly a result of conditions during the last glaciation. We note that the deepest part (>650 m) is at the shelf edge rather than farther inboard, as is the case of the largest Antarctic ice streams like the Amery and Filchner ice shelves. These Antarctic ice streams have over-deepened troughs extending to 800 and 1100 m present water depth, respectively, but are terminated at the shelf edge by a sill shallower than 600 m present water depth. The morphology of the St. Anna Trough suggests that glacier input from the Kara Sea or at least some past Kara-Barents Sea ice sheets was probably more significant than the "maximum sized" alternative suggested by numerical modeling of the late Weichselian situation [*Siegert and Dowdeswell*, 1999; *Dowdeswell and Siegert*, 1999]. Alternatively, more focused ice flow may have eroded a deeper trough. Glacial troughs on the Canadian Arctic margin such as the Amundsen Gulf and McClure Strait are eroded to maximum 450 m present water depth. Icebergs discharged from this area into the Arctic Ocean would have less extreme drafts, which is reflected in the shallower depth of iceberg scouring on Northwind Ridge and Chukchi Plateau [*Polyak et al.*, 2001].

[27] Floating ice shelves or glacier tongues, which extend seaward from a grounded ice sheet, show a quasi-cyclic pattern of calving followed by growth [*Holdsworth and Glynn*, 1981]. Antarctic icebergs with areas up to 10,000 km^2 drift intact for several years [*Swithinbank et al.*, 1977; *Fricker et al.*, 2002]. However, the draft of these giants is less than 500 m (typically 300 m), partly because of the free seaward boundary of the tabular ice shelves and also because of melting within subice cavities [*Fricker et al.*, 2002; *Jacobs et al.*, 1992]. Generation of thicker icebergs require back pressure from buttressing thresholds or pinning points. To achieve an iceberg thickness of +800 m requires input by fast convergent glacier flow and a calving front close to the grounding line [*Stokes and Clark*, 2001]. The most likely mechanisms for destabilizing an ice sheet is rapid sea level rise during deglaciations or delayed glacio-isostatic subsidence in the grounding line region during maximum ice sheet growth [*Hughes*, 1987]. The lack of a sill in St. Anna Trough would favor rapid draw-down of an ice sheet on the Kara-Barents Sea continental margin to provide the deepest draft glacier input to the Arctic Ocean. The discharge event(s) must have involved high ice stream velocities if we draw on analogies from the model of a late Weischelian "maximum-sized" Eurasian High Arctic ice sheet by *Siegert and Dowdeswell* [1999]. The distance from the shelf edge in the St. Anna Trough to where the model ice sheet reach +800 m thickness is more than 300 km.

4.3. Ice Dynamics and Paleocirculation

[28] Some of the deep draft glacier ice which exited the Arctic Ocean through the Fram Strait moved diagonally across Yermak Plateau from northeast to southwest. In the central Arctic Ocean the thickest ice moved in an eastward direction across Lomonosov Ridge into the Makarov Basin [*Polyak et al.*, 2001] or turned southeast where constrained by local seafloor topography (Figure 1). Published seismic reflection profiles from north of De Long Island (Figure 1) and the Laptev Sea margin [*Sekretov*, 2001, 2002] appear inconclusive as to the presence of similar changes in seabed morphology as observed on Yermak Plateau around 850 m and associated with the depth limit of iceberg contact with the seabed.

[29] The wind-driven surface circulation in the Arctic Ocean under the present interglacial conditions is characterized by the by the Transpolar Current in the Eurasia Basin and the clockwise Beaufort Gyre in the Canada Basin. Warm Atlantic water enters the Eurasia Basin in roughly equal volumes through the Fram Strait and through the Kara-Barents Sea with an eastward flow (Figure 1) opposite the surface circulation [*Rudels et al.*, 1994; *Karcher and Oberhuber*, 2002]. The Atlantic water encompasses the depth range 200–800 m with a core at ~300 m (Figure 1) and velocities of 1–5 cm/s [*Zhang et al.*, 1998; *Woodgate et al.*, 2001]. Included in the eastward flow is also a mixed layer above the Atlantic layer so that the entire water column below 50 m depth north of the Kara-Barents Sea margin is flowing east and north [*Rudels et al.*, 1996]. In the Canada Basin the intermediate depth waters between 200 and 1700 m flow east north of Alaska and Canada opposite to surface flow in the Beaufort Gyre [*Karcher and Oberhuber*, 2002; *Rudels et al.*, 1994; *McLaughlin et al.*, 2002].

[30] During glacial times, the presence of ice sheets in the Barents and Kara Seas would confine all inflow of Atlantic water into the Arctic Ocean through the Fram Strait. At the Fram Strait gateway, analysis of a relatively high-resolution paleoenvironmental record from ODP sites 909 and 912 extending back to MIS 12 show glaciations during isotope stages 6 and 12 to be more severe than the last glaciation [*Hevrøy et al.*, 1996]. The trend in the content of foraminifers is toward more open water with a higher production during the last two glacial/interglacial cycles [*Lloyd et al.*, 1996; *Hebbeln and Wefer*, 1997; *Spielhagen et al.*, 2004].

North of Svalbard the core of Atlantic water turns east and follows the continental slope between Yermak Plateau and Severnaya Zemlya (Figure 1). The few short sediment cores available from the area document advection of surface and/or subsurface Atlantic water coupled with seasonally ice-free conditions during the last 150 kyr to at least the Franz-Victoria Trough west of Franz Josef Land [*Knies et al.*, 2000; *Matthiessen et al.*, 2001]. The strongest advection occurred during substages 6.3, 5.5, 5.1 and the Holocene [*Knies et al.*, 1999, *Wollenburg et al.*, 2001]. Paleoproductivity estimates of benthic foraminifera in a sediment core from 995 m water depth in this area representing the last 145 kyr are all higher than values from the modern ice-covered Arctic Ocean [*Wollenburg et al.*, 2001]. Thus the large-scale oceanic circulation at least in the Eurasia Basin may have varied in strength between glacial and interglacial times, but there are no compelling arguments for assuming major differences in the circulation pattern.

[31] The drift of deep draft icebergs is determined by the sum of forces acting on their surface areas. An iceberg in the Eurasian Basin with a thickness of more than 600 m would have more than 90% of its draft submerged in the Atlantic layer (Figure 1). Although the current velocities below the fresh surface layer (~50 m depth) are lower than surface velocities [*Zhang et al.*, 1998; *Woodgate et al.*, 2001], the current stresses would act over a much larger area and in some cases would be sufficient to control iceberg motion. The direction of iceberg drift would depend on the draft. Icebergs discharged from the northern margin of ice sheets in the Kara-Barents Sea with drafts which included most of Atlantic layer would probably drift east and north, whereas the trajectory of bergs with shallow draft would be determined by the wind driven surface current and exit the Fram Strait closer to Svalbard (Figure 1). A northern trajectory for the deepest draft icebergs from this source area is also corroborated by lack of evidence in the seabed morphology for a pile-up of the deepest icebergs in the bight at the junction between Yermak Plateau and the continental slope north of Svalbard, resulting from a drift trajectory mainly controlled by the surface circulation (Figures 1 and 4). A stronger Atlantic inflow would favor exit of icebergs more to the west in the central Fram Strait and leave fewer imprints on the seabed on Yermak Plateau.

[32] Qualitative information on past motion of marine ice is carried in the abundance, grain-size distribution, and lithology of ice-rafted detritus (IRD) deposited on the seabed. Sediments entrained in sea ice tend to be fine-grained particles from coastal environments [*Nürnberg et al.*, 1994], while glacier ice may contain all grain sizes [*Clark and Hanson*, 1983]. However, the temporal and spatial relations between IRD sources, abundances, and phases of the glacial-interglacial cycles of particular interest here (MISs 16, 12, and 6) are not well understood despite much study [*Bischof et al.*, 1996; *Bischof and Darby*, 1997]. *Spielhagen et al.* [2004] associate elevated smectite contents of IRD-rich sediments deposited during MIS 6 on Lomonosov Ridge (Figure 2, core PS2185) with a possible source area in the eastern Kara Sea/western Laptev Sea. Coal fragments constitute between 20 and 65% of ice rafted debris >0.5 mm in the Eurasia Basin, Fram Strait, and the eastern Norwegian-Greenland Sea in sediments from oxygen isotope stage 6. Only subordinate amounts are present in sediments from stages 1 to 5 [*Bischof et al.*, 1990]. Comparison of vitrinite reflectance values suggests that the source of the coal may be low-rank coals from Franz Josef Land, northern Siberia, or Taymyr Peninsula. Coal is also abundant in IRD for glacial stages 8, 10, and 12 in the Fram Strait [*Hevrøy et al.*, 1996], suggesting discharge of ice from a Kara-Barents ice sheet.

[33] Support for a persistent late Quaternary oceanic circulation pattern comes from analysis of glacial erratics in 27 box cores and 7 piston cores which form a transpolar transect from the Chukchi Sea to the Eurasia Basin. *Philips and Grantz* [2001] define a distinct Amerasia Basin suite (dolostone and limestone) and an abrupt change at the position of Lomonosov Ridge to a Eurasia Basin suite (siltstone, sandstone, and siliceous clasts) of glacial erratics. The carbonate-rich Paleozoic terranes of the Canadian Arctic Islands are the likely source of the Amerasia suite [*Bischof et al.*, 1990], while the source for the Eurasia Basin suite is not well defined but considered to be the Taimyr Peninsula–Kara Sea region.

4.4. Timing of Deep Draft Iceberg Erosion Events

[34] Icebergs in the polar basin would eventually exit the Arctic Ocean through the Fram Strait gateway and would be likely to impact the seafloor sediments on Yermak Plateau. Sites 910–912 of the Ocean Drilling Program constitute a transect across southern Yermak Plateau (Figure 4). Two of the sites (911 and 912) were drilled on the flanks at or just below the maximum water depth of ice disturbance (Figure 5). Site 910 on the plateau crest yielded over-consolidated sediments from ~19 to 70–95 m below the seafloor [*Thiede and Myhre*, 1996]. Over-consolidation was attributed to enhanced compaction of sediments beneath an ice sheet extending north from Svalbard prior to MIS 16 (~660 ka) [*Flower*, 1997]. The biostratigraphy suggests a hiatus in the lower part of the over-consolidated section, where much of the lower Quaternary to upper Pliocene sediments are missing [*Hull et al.*, 1996]. We infer that deep draft icebergs exiting the polar basin removed this part of the stratigraphy prior to and/or during MIS 16 and redeposited the material as a wedge to the west (Figure 5). Although subsequent deposition appears continuous, the lack of coherent acoustic stratification in the post-MIS 16 unit, as well as plowmarks on the modern seabed, strongly suggests that keels of isolated icebergs have subsequently interacted with the seabed down to water depths equivalent to the deepest erosion level on northern Yermak Plateau. High pre-MIS 6 concentrations of ice-rafted detritus on Yermak Plateau suggest that earlier glaciations (MISs 6–12) were more severe than the last one [*Hevrøy et al.*, 1996]. On Lomonosov Ridge a piston core (Figure 2, core 9609pc) recovered undisturbed sediments not older than MIS 6 overlying consolidated material at the uppermost erosional unconformity [*Jakobsson et al.*, 2001]. This apparent discrepancy in the timing of erosion by thick glacier ice in the Arctic Ocean may have several explanations such as: local areas were affected at different

times, or glacier ice eroded both Lomonosov Ridge and Yermak Plateau just prior to MIS 16, but pre-MIS 6 deposits were removed at the particular coring location on Lomonosov Ridge.

[35] Northward motion of deep draft glacier ice discharged into the Eurasia Basin would depend on the relative strength of flow in the Atlantic layer, and only icebergs with drafts which exceeded thresholds on Lomonosov Ridge would leave a legacy by eroding the seabed. We propose that intensified advection of Atlantic water at least during surges or collapse of the Saalian ice sheet facilitated northward drift of deep draft icebergs across Lomonosov Ridge from discharge areas along the northern Kara-Barents Sea margin. Better time resolution of erosion events on Lomonosov Ridge would tell whether or not forcing from subsurface Atlantic inflow at times not necessarily associated with open water conditions along the northern Kara-Barents Sea margin was sufficient to drive icebergs far to the north. Ice that reached the central Arctic Ocean would exit the polar basin in the central part of the Fram Strait, as would icebergs originating from the Canada/Alaska margin and the Chuckchi area. This ice export would largely bypass Yermak Plateau (Figure1). The oceanographic situation during MIS 16 was possibly different where weaker inflow of Atlantic water gave reduced northward drift with limited iceberg impact on Lomonosov Ridge but a large ice flux across Yermak Plateau. Although we cannot exclude the possibility of the MIS 6 seabed erosion on Lomonosov Ridge being caused during brief maximum advance of a floating, continuous ice sheet extending from the Kara-Barents Sea margin [*Jakobsson et al.*, 2003], we would have expected a contemporary massive impact on Yermak Plateau from its decay, which is not documented in the available data [*Flower*, 1997]. The record for MIS 6 shows strong IRD input interrupted by short-term advection of Atlantic water during which seasonally ice-free conditions existed in the Fram Strait [*Lloyd et al.*, 1996; *Hebbeln and Wefer*, 1997; *Knies et al.*, 1999]. Farther east, northeast of Svalbard, MIS 6 include three IRD peaks, the first one related to MIS event 6.3 [*Knies et al.*, 2001]. The MIS 6/5 transition is associated with strong IRD along the northern margin, at least as far east as Severnaya Zemlya [*Knies et al.*, 2001], suggesting the collapse of the Kara Sea component of the extensive Saalian ice cover [*Arkhipov et al.*, 1995].

4.5. Climatic Significance of Deep Draft Ice in the Polar Basin

[36] The paleoceanographic evidence suggests unrestricted ice export from the polar basin through the Fram Strait prevailed during glacial extremes including MIS 12 [*Hevrøy et al.*, 1996; *Hebbeln and Wefer*, 1997]. In the modern Arctic Ocean, undeformed sea ice reaches a thermodynamic equilibrium thickness of 2.5–5 m [*Weeks and Ackley*, 1986]. Sea ice is concentrated by wind stresses and thickened by deformation to more than 7 m north of the Canadian Arctic and Greenland [*Bourke and Garrett*, 1987]. Lower temperatures during glacial extremes would only yield a slight increase in the equilibrium average sea ice thickness. Deep draft ice in the Arctic Ocean must have come from the surrounding grounded marine or land-based ice sheets and as such does not represent a separate contribution in the global oxygen isotope record, but rather an increase in sea level [*Broecker*, 1975; *Williams et al.*, 1981; *Shackleton*, 1987]. The relative strength of inflow of Atlantic water would determine how far the iceberg armada would penetrate into the central Arctic Ocean, such as evidently was the case at least at the end of or during MIS 6 [*Jakobsson et al.*, 2001]. Under present interglacial conditions the entire water column below 50 m depth would contribute to eastward and northward directed drift if any deep draft icebergs were present. The actual drift trajectory of an iceberg and its legacy imprinted on the seabed would depend on its draft.

[37] Massive release of icebergs into the Arctic Ocean would potentially create recognizable equivalents of Henrich layers, depending of how contracted these events were as well as the position of the icebergs at the time detritus was released. To this point, *Knies et al.* [2001] have identified distinct events of IRD deposition (SB2 and SB3) north of Svalbard/Barents Sea contemporary to the North Atlantic Heinrich Events H2 and H3. Also, the IRD content in a sediment core from northeast Greenland continental slope (1235 m water depth) in the Fram Strait reveals four distinct episodes between 14 and 34 ka of increase in the abundance of iron oxide grains [*Darby et al.*, 2002]. A discriminant function analysis of circum-Arctic source area samples identifies the Laurentide and the Innutian ice sheets as the origin of the IRD carrier and suggests rapid purges of glacier ice through the Fram Strait but at times most likely preceding North Atlantic Heinrich events [*Darby et al.*, 2002]. Pre-Weischelian glacial purges are likely to have been far more dramatic than the late Weischelian events detected so far but remain unobserved in the present inventory of sediment cores from the Eurasia Basin. Melt-out of basal detritus from deep draft ice below the main influence of warm Atlantic water could to some extent be delayed until exit of the Arctic Ocean.

5. Conclusions

[38] Evaluation of available seismic data demonstrates that some of the deepest draft glacier ice which reached the central Arctic Ocean traversed the Lomonosov Ridge from the Eurasia Basin. The ice was in the form of large isolated icebergs with limited momentum as it eroded and peneplained ridge topography, which were maybe 50 m shallower than maximum draft ($\sim$980 m present water depth) but was deviated by thicker (up to 300 m shallower) unconsolidated sediments. The existence of uneroded pelagic sediments on the Amerasian flank of the Lomonosov Ridge demonstrates that there was no continuous sheet of thick ice blanketing the Arctic Ocean. The Lomonosov Ridge was in part a barrier to the eroding ice, which had its probable source on the Kara-Barents shelves. Given the present morphology of the continental shelf, thick ice was probably delivered to the Arctic Ocean through the St. Anna Trough. The thickest icebergs imply rapid drawdown from large ice sheets, most likely during deglaciation events. Paleoceanographic

data suggest that the basic circulation pattern has persisted at least throughout the last 400 kyr with varying inflow of Atlantic water into the Arctic Ocean during all glacial periods [*Hevrøy et al.*, 1996; *Hebbeln and Wefer*, 1997; *Knies et al.*, 1999]. Northward drift of deep draft icebergs may be considered a proxy for the relative strength of Atlantic inflow at the particular time of iceberg discharge, but the documentation is restricted to events when iceberg drafts exceeded bathymetric thresholds on Lomonosov Ridge. At least one erosion event occurred on the ridge during MIS 6 [*Jakobsson et al.*, 2001]. Subsurface Atlantic inflow may have been sufficiently strong to drive icebergs northward at times not directly associated with open water conditions along the northern margin. Erosion by deep draft ice in the central Arctic Ocean as well as drift trajectories controlled by Atlantic inflow appear to directly reflect the change toward more extensive glaciations and increased warm water advection following the Mid-Pleistocene Revolution [*Berger and Jansen*, 1994]. Future high-resolution seismic surveys and a east-west transect with sediment sampling by continuous coring of the upper ~200 m of subbottom sediments on Yermak Plateau may provide the most complete history of release of deep draft icebergs into the Eurasia Basin.

[39] **Acknowledgments.** We thank the officers and the crew of R/V *Helland-Hansen* (1976–1979), *Polarstern* (1991), *Oden* (1996), and the U.S. Navy's nuclear submarine *Hawkbill* (1999) for their contribution to acquisition of challenging data sets. The effort of Erik Sundvor in acquiring the early seismic data is much appreciated, and Øyvind Engen kindly provided sonobuoy velocity information. We enjoyed stimulating discussions with M. Jakobsson and A. Grantz and thank A. Elverhøi and Jan Mangerud for critical comments on the original manuscript. This research was funded by the Norwegian Research Council, the Norwegian Petroleum Directorate, Alfred-Wegener Institute of Marine and Polar Research, and the U.S. National Science Foundation. Figures were generated using the GMT software [*Wessel and Smith*, 1991].

References

Aagaard, K. (1981), On the deep circulation in the Arctic Ocean, *Deep Sea Res. Part A*, *28*, 251–268.

Aldahan, A. A., S. Ning, G. Possnert, J. Backman, and K. Boström (1997), ^{10}Be records from sediments of the Arctic Ocean covering the past 350 ka, *Mar. Geol.*, *144*, 147–162.

Arkhipov, S. A., J. Ehlers, R. G. Johnson, and H. E. Wright Jr. (1995), Glacial drainage towards the Mediterranean during the middle and late Pleistocene, *Boreas*, *24*, 196–206.

Austegard, A. (1982), Velocity analysis of sonobuoy data from the northern Svalbard margin, *Sci. Rep. 9*, 26 pp., Seismol. Obs., Univ. of Bergen.

Berger, W. H., and E. Jansen (1994), Mid-Pleistocene climate shift—The Nansen connection, in *The Polar Oceans and Their Role in Shaping Global Environment: The Nansen Centennial Volume*, *Geophys. Monogr. Ser.*, vol. 85, edited by O. M. Johannessen, R. D. Munch, and J. E. Overland, pp. 295–311, AGU, Washington, D. C.

Bischof, J., and D. Darby (1997), Mid- to late Pleistocene ice drift in the western Arctic Ocean: Evidence of a different circulation in the past, *Science*, *277*, 74–78.

Bischof, J., J. Koch, M. Kubisch, R. F. Spielhagen, and J. Thiede (1990), Nordic Seas surface ice drift reconstructions: Evidence from ice rafted coal fragments during oxygen isotope stage 6, in *Glaciomarine Environments: Processes and Sediments*, *Geol. Soc. Spec. Publ.*, vol. 53, edited by J. A. Dowdeswell and J. D. Scourse, pp. 235–251, Geol. Soc., London.

Bischof, J., D. L. Clark, and J.-S. Vincent (1996), Origin of ice-rafted debris: Pleistocene paleoceanography in the western Arctic Ocean, *Paleoceanography*, *11*, 743–756.

Blasco, S. M., B. D. Bornhold, and C. F. M. Lewis (1979), Preliminary results of surficial geology and geomorphology studies of the Lomonosov Ridge, central Arctic Ocean, *Pap. Geol. Surv. Can.*, *79-1C*, 73–83.

Boström, K., and J. Thiede (1984), Ymer-80: Cruise report for marine geology and geophysics with sediment core descriptions, *Meddl. 260*, 123 pp., Geol. Inst., Stockholm Univ., Stockholm.

Bourke, R. H., and R. P. Garrett (1987), Sea ice thickness distribution in the Arctic Ocean, *Cold Regions Sci. Technol.*, *13*, 259–280.

Broecker, W. S. (1975), Floating glacial ice caps in the Arctic Ocean, *Science*, *188*, 1116–1118.

Cherkis, N., et al. (1991), *Bathymetry of the Barents and Kara Seas*, Geol. Soc. of Am., Boulder, Colo.

Clark, D. L. (1990), Arctic Ocean ice cover: Geologic history and climatic significance, in *The Geology of North America*, vol. L, *The Arctic Ocean Region*, edited by A. Grantz, L. Johnson, and J. F. Sweeney, pp. 53–63, Geol. Soc. of Am., Boulder, Colo.

Clark, D. L., and A. Hanson (1983), Central Arctic Ocean sediment texture: A key to ice-transport mechanism, in *Glacial-Marine Sedimentation*, edited by B. Molnia, pp. 301–330, Plenum, New York.

Darby, D. A., J. F. Bischof, R. F. Spielhagen, S. A. Marshall, and S. W. Herman (2002), Arctic ice export events and their potential impact on global climate during the late Pleistocene, *Paleoceanography*, *17*(2), 1025, doi:10.1029/2001PA000639.

Dowdeswell, J., and M. Siengert (1999), Ice-sheet numerical modelling and marine geophysical measurements if glacier derived sedimentation on the Eurasian Arctic continental margins, *Geol. Soc. Am. Bull.*, *111*, 1080–1097.

Evans, J. R., and M. A. Kaminski (1998), Pliocene and Pleistocene chronostratigraphy and paleoenvironment of the central Arctic Ocean, using deep water agglutinated foraminifera, *Micropaleontology*, *44*, 109–130.

Flower, B. P. (1997), Overconsolidated section on the Yermak Plateau, Arctic Ocean: Ice sheet grounding prior to ca. 660 ka?, *Geology*, *25*, 147–150.

Fricker, H. A., N. W. Yound, I. Allison, and R. Coleman (2002), Iceberg calving from the Amery Ice Shelf, east Antarctica, *Ann. Glaciol.*, *34*, 241–246.

Grosswald, M., and T. J. Hughes (1999), The case for an ice shelf in the Pleistocene Arctic Ocean, *Polar Geogr.*, *23*, 23–54.

Hebbeln, D., and G. Wefer (1997), Late Quaternary paleoceanography in the Fram Strait, *Paleoceanography*, *12*, 65–78.

Hevrøy, K., G. Lavik, and E. Jansen (1996), Quaternary paleoceanography and paleoclimatology of the Fram Strait/Yermak Plateau region: evidence from Sites 909 and 912, *Proc. Ocean Drill. Program Sci. Results*, *151*, 469–482.

Holdsworth, G., and J. E. Glynn (1981), A mechanism for the formation of large icebergs, *J. Geophys. Res.*, *86*, 3210–3222.

Hughes, T. (1987), Ice dynamics and degalciation models when ice sheets collapsed, in *North America and Adjacent Oceans During the Last Deglaciation*, edited by W. F. Ruddiman and H. E. Wright Jr., pp. 183–220, Geol. Soc. of Am., Boulder, Colo.

Hughes, T., J. F. Denton, and M. G. Grosswald (1977), Was there a late-Würm Arctic Ice Sheet?, *Nature*, *266*, 596–602.

Hull, D. L., I. E. Osterman, and J. Thiede (1996), Bio-stratigraphic synthesis of Leg 151, North Atlantic-Arctic gateways, *Proc. Ocean Drill. Program Sci. Results*, *151*, 627–644.

Ishman, S. E., L. Polyak, and R. Z. Poore (1996), Expanded record of Quaternary oceanographic change: Amerasian Arctic Ocean, *Geology*, *24*, 139–142.

Jacobs, S., H. H. Helmer, C. S. M. Doake, A. Jenkins, and R. M. Frolich (1992), Melting of ice shelves and the mass balance of Antarctica, *J. Glaciol.*, *38*, 375–387.

Jakobsson, M. (1999), First high-resolution chirp sonar profiles from the central Arctic Ocean reveal erosion of Lomonosov Ridge sediments, *Mar. Geol.*, *158*, 11–123.

Jakobsson, M. (2000), Mapping the Arctic Ocean: Bathymetry and Pleistocene paleoceanography, *Meddl. 306*, 68 pp., Stockholm Univ., Stockholm.

Jakobsson, M., N. Cherkis, J. Woodward, R. Macnab, and B. Coakley (2000), New grid of Arctic bathymetry aid scientists and mapmakers, *Eos Trans. AGU*, *81*, 89, 93, 96.

Jakobsson, M., R. Løvlie, E. M. Arnold, J. Backman, L. Polyak, J. O. Knutsen, and E. Musatov (2001), Pleistocene stratigraphy and paleoenvironmental variation from Lomonosov Ridge sediments, central Arctic Ocean, *Global Planet. Change*, *31*, 1–22.

Jakobsson, M., M. J. Siegert, and M. Paton (2003), On the grounding of an ice shelf in the central Arctic Ocean: A modeling experiment (abstract), paper presented at International Conference on Arctic Margins, Geol. Soc. of Can., Dartmouth, Nova Scotia.

Jokat, W., G. Uenzelmann-Neben, Y. Kristoffersen, and T. M. Rasmussen (1992), Lomonosov Ridge—A double-sided continental margin, *Geology*, *20*, 887–890.

Karcher, M. J., and J. M. Oberhuber (2002), Pathways and modification of the upper and intermediate waters of the Arctic Ocean, *J. Geophys. Res.*, *107*(C6), 3049, doi:10.1029/2000JC000530.

Knies, J., C. Vogt, and R. Stein (1999), Late Quaternary growth and decay of the Svalbard/Barents Sea ice sheet and paleocanographic evolution in the adjacent Arctic Ocean, *Geo Mar. Lett.*, *18*, 195–202.

Knies, J., N. Nowaczyk, C. Müller, C. Vogt, and R. Stein (2000), A multiproxy approach to reconstruct the environmental changes along the Eurasian continental margin over the last 150,000 years, *Mar. Geol.*, *163*, 317–344.

Knies, J., H.-P. Calibre, J. Matheson, C. Muller, and N. Nowaczyk (2001), Marine ice-rafted debris records constrain maximum extent of Salian and Weischelian ice-sheets along the northern Eurasia margin, *Global Planet. Change*, *31*, 45–64.

Lloyd, J. M., D. Kroon, G. S. Boulton, C. Laban, and A. Fallick (1996), Ice rafting history from the Spitsbergen ice cap over the last 200 kyr, *Mar. Geol.*, *131*, 103–121.

Mathiessen, J., J. Knies, N. Nowaczyk, and R. Stein (2001), Late Quaternary dinoflaggelate cyst stratigraphy at the Eurasian continental margin, Arctic Ocean: Indications for Atlantic water inflow in the past 150,000 years, *Global Planet. Change*, *31*, 65–86.

McLaughlin, F., E. Carmack, R. Macdonald, A. J. Weaver, and J. Smith (2002), The Canada Basin, 1989–1995: Upstream events and far-field effects of the Barents Sea, *J. Geophys. Res.*, *107*(C7), 3082, doi:10.1029/2001JC000904.

Mercer, J. H. (1970), A former ice sheet in the Arctic Ocean, *Palaeogeogr. Palaeoclimatol. Palaecol.*, *8*, 19–27.

Myhre, A. M., et al. (1995), *Proceedings of the Ocean Drilling Program Initial Reports*, vol. 151, Ocean Drill. Program, College Station, Tex.

Nürnberg, D., I. Wollenburg, D. Dethleff, H. Eicken, H. Kassens, T. Letzig, E. Reimnitz, and J. Thiede (1994), Sediments in Arctic sea-ice: Implication for entrainment, transport and release, *Mar. Geol.*, *119*, 185–214.

Philips, R. L., and A. Grantz (2001), Regional variations in provenance and abundance of ice rafted clasts in Arctic Ocean sediments: Implications for the configuration of late Quaternary oceanic and atmospheric circulation in the Arctic, *Mar. Geol.*, *172*, 91–115.

Polyak, L., M. Edwards, B. Coakley, and M. Jakobsson (2001), Ice shelves in the Pleistocene Arctic Ocean inferred from glacigenic deep-sea bedforms, *Nature*, *410*, 453–457.

Reeh, N., H. Højmark Thomsen, A. K. Higgins, and A. Weidick (2001), Sea ice and the stability of north and northeast Greenland floating glaciers, *Ann. Glaciol.*, *33*, 474–480.

Rigor, I. G., J. Wallace, and R. L. Colony (2002), On the response of sea ice to the Arctic Oscillation, *J. Clim.*, *15*, 2648–2668.

Rohling, E. J., M. Fenton, F. J. Jorissen, P. Bertrand, G. Ganssen, and J. P. Caulet (1998), Magnitudes of sea-level lowstands of the past 500,000 years, *Nature*, *394*, 162–165.

Rudels, B., E. P. Jones, L. G. Anderson, and G. Kattner (1994), On the intermediate depth waters of the Arctic Ocean, in *The Polar Oceans and Their Role in Shaping the Global Environment: The Nansen Centennial Volume*, *Geophys. Monogr. Ser.*, vol. 85, edited by O. M. Johannessen, R. D. Munch, and J. E. Overland, pp. 33–46, AGU, Washington, D. C.

Rudels, B., L. G. Anderson, and E. P. Jones (1996), Formation and evolution of the surface mixed layer and halocline of the Arctic Ocean, *J. Geophys. Res.*, *101*, 8807–8821.

Sekretov, S. B. (2001), Northwestern margin of the east Siberian Sea, Russian Arctic: Seismic stratigraphy, structure of the sedimentary cover and some remarks on the tectonic history, *Tectonophysics*, *339*, 353–383.

Sekretov, S. B. (2002), Structure and tectonic evolution of the southern Eurasia Basin, Arctic Ocean, *Tectonophysics*, *351*, 193–243.

Shackleton, N. J. (1987), Oxygen isotopes, ice volume and sea level, *Quat. Sci. Rev.*, *6*, 183–190.

Siegert, M., and J. A. Dowdeswell (1999), Late Weischelian glaciation of the Russian high Arctic, *Quat. Res.*, *52*, 273–285.

Spielhagen, R., K.-H. Baumann, H. Erlenkeuser, R. Nowaczyk, N. Nørgaard-Pedersen, C. Vogt, and D. Weiel (2004), Arctic Ocean deep-sea record of northern Eurasian ice sheet history, *Quat. Sci.*, *23*, 1455–1483.

Stokes, C. R., and C. D. Clark (2001), Palaeo-ice streams, *Quat. Sci. Rev.*, *20*, 1437–1457.

Sundvor, E., A. M. Myhre, A. Austegard, K. Haugland, O. Eldholm, and A. Gidskehaug (1982), Marine geophysical survey on the Yermak Plateau, *Sci. Rep. 7*, 29 pp., Seismol. Obs., Univ. of Bergen, Bergen.

Swithinbank, C., P. McClain, and P. Little (1977), Drift tracks of Antarctic icebergs, *Polar Rec.*, *18*, 495–501.

Thiede, J., and A. Myhre (1996), The paleoceanographic history of the North Atlantic-Arctic gateways: Synthesis of the Leg 151 drilling results, *Proc. Ocean Drill. Program Sci. Results*, *151*, 645–658.

Vogt, P. R., K. Crane, and E. Sundvor (1994), Deep Pleistocene iceberg plowmarks on the Yermak Plateau: Sidescan and 3.5 kHz evidence for thick calving ice fronts and a possible marine ice sheet in the Arctic Ocean, *Geology*, *22*, 403–406.

Weber, J. R. (1980), Exploring the Arctic seafloor, *GEOS*, *9*, 2–7.

Weeks, W. F., and S. F. Ackley (1986), The growth, structure, and properties of sea ice, *CRREL Monogr. 82–1m*, Cold Regions Res. and Eng. Lab., Hanover, N. H.

Wessel, P., and W. H. F. Smith (1991), Free software helps map and display data, *Eos Trans AGU*, *72*, 441, 445–446.

Williams, D. F., W. S. Moore, and R. H. Fillon (1981), Role of glacial Arctic Ocean ice sheet in Pleistocene oxygen isotope and sea level records, *Earth Planet. Sci. Lett.*, *56*, 157–166.

Wollenburg, J., W. Kuhn, and A. Mackenzie (2001), Changes in Arctic Ocean paleoproductivity and hydrograph during the last 145 kyr: The benthic foraminiferal record, *Paleoceanography*, *16*, 65–77.

Woodgate, R., K. Aagard, R. D. Muench, J. Gunn, G. Björk, B. Rudels, A. T. Roach, and U. Schauer (2001), The Arctic Ocean boundary current along the Eurasian slope and the adjacent Lomonosov Ridge: Water mass properties, transports and transformations from moored instruments, *Deep Sea Res.*, *Part I*, *48*, 1757–1792.

Zhang, J., D. A. Rothrock, and M. Steele (1998), Warming of the Arctic Ocean by a strengthened Atlantic inflow: Model results, *Geophys. Res. Lett.*, *25*, 1745–1748.

H. Brekke, Norwegian Petroleum Directorate, P.O. Box 600, N-4003 Stavanger, Norway.

B. Coakley, Department of Geology and Geophysics, University of Alaska, Fairbanks, AK 99775-5780, USA.

M. Edwards, Hawaii Mapping Research Group, Hawaii Institute of Geophysics and Planetology, University of Hawaii, Honolulu, Hawaii 96822, USA.

J. Gjengedal and Y. Kristoffersen, Department of Earth Science, University of Bergen, N-5007 Bergen, Norway. (yngve.kristoffersen@geo.uib.no)

W. Jokat, Alfred-Wegener Institute for Marine and Polar Research, Columbusstrasse, D-27568 Bremerhaven, Germany.